J Therm Anal Calorim (2013) 113:1497–1503
DOI 10.1007/s10973-012-2934-x

Computational prediction of the pattern of thermal gravimetry data for the thermal decomposition of calcium oxalate monohydrate

J. Błażejowski · B. Zadykowicz

Received: 31 October 2012 / Accepted: 21 December 2012 / Published online: 12 February 2013

Abstract The multistep decomposition of $CaC_2O_4 \cdot H_2O$ in the gaseous phase was explored at the MP2/cc-pVDZ level of theory. As a result, the structure and energy of the entities occurring at stationary points along the reaction pathway were determined. Statistical thermodynamics routines were used to obtain thermal energies/enthalpies and entropies. The results demonstrated the consecutive release of H_2O, CO and CO_2 from the substrate with increasing temperature. Moreover, the application of thermodynamic and kinetic characteristics to relevant phenomenological relationships enabled the decomposition pattern in equilibrium and non-equilibrium conditions to be predicted. The forecast patterns qualitatively match the experimental thermal gravimetry data. This study supplies much important information on the molecular changes taking place in a stoichiometric unit of calcium oxalate monohydrate during continuous heating

Keywords Calcium oxalate monohydrate · Ab initio calculations · Decomposition pattern prediction · Thermodynamic and kinetic analysis · Computational versus experimental TG data

Introduction

Calcium oxalate monohydrate is a well-known, standard material in thermal analysis investigations [1–9]. For this reason many authors have included studies on the features and reactivity of this compound in their research projects. Some thermal analysis papers tackle the chemical and energetic changes that take place during continuous heating [1], while others touch on the kinetics of the compound's thermal decomposition [2–9]. To our knowledge, only a few papers have been published in which computational methods are used to explore the behaviour and reactivity of $CaC_2O_4 \cdot H_2O$ and the related compound [1, 10, 11]. Among them is one of our papers [1], in which the decomposition of calcium oxalate monohydrate was studied at a lower level of theory than in the present paper. Sixteen years have elapsed since the publication of that work, so we thought that it would be interesting to carry out new quantum chemistry calculations, at one of the most advanced levels of theory nowadays available, for a single $CaC_2O_4 \cdot H_2O$ unit and conglomerates of such units simulating a solid phase (an issue not yet completely explored), in order to predict the thermal behaviour of the compound during continuous heating in equilibrium and non-equilibrium conditions. This study focuses on predicting the course of thermal decomposition of $CaC_2O_4 \cdot H_2O$ in the gaseous phase and the shape of the thermal gravimetry (TG) curves, and compares patterns of predicted and experimental TG data.

Methods

Material

High purity calcium oxalate monohydrate (puratronic, 99.9985 %) was purchased from Alfa Aesar and used as received.

This paper is part of 'The 2012 TA Instruments-ICTAC Award' lecture presented at the 15th ICTAC Congress in Osaka, Japan, in August 2012.

J. Błażejowski (✉) · B. Zadykowicz
Faculty of Chemistry, University of Gdańsk, J. Sobieskiego 18, 80-952 Gdańsk, Poland
e-mail: bla@chem.univ.gda.pl

TG measurements

Thermal gravimetry measurements were carried out on a Netzsch STA 449 F3 thermobalance. Samples weighing 12.0 or 14.2 mg were placed in a platinum crucible and heated at 5.0 and 25.0 K min^{-1} in a dynamic Ar atmosphere.

Quantum chemistry and thermodynamic computations

Unconstrained geometry optimizations of isolated entities ($CaC_2O_4{\cdot}H_2O$, CaC_2O_4, $CaCO_3$, CaO, H_2O, CO and CO_2) in the lowest-energy and transition (TS) states for decomposition ($CaC_2O_4{\cdot}H_2O$, CaC_2O_4, $CaCO_3$) were carried out at the MP2 level of theory [12] using the cc-pVDZ basis set [13, 14] and the Gaussian 09 program package [15]. Structures of $CaC_2O_4{\cdot}H_2O$, CaC_2O_4 and $CaCO_3$ for optimizations were initially extracted from relevant crystallographic data [16–18]. The validity of the geometry optimizations was demonstrated in the subsequent Hessian (second derivatives of the energy versus nuclear coordinates) calculations followed by normal mode analyses [19]. The bond lengths and vibrational harmonic frequencies so determined were then used to obtain the zero-point energy, entropy (${}_TS^\circ$), thermal enthalpy and Gibbs free energy contributions at 298.15 K and standard pressure (°) applying a built-in computational program of statistical thermodynamics routines [20]. On the basis of these data, the sum (denoted ${}_TH^\circ$) of energy corresponding to the optimized structure, zero-point energy and thermal enthalpy contribution and the sum (denoted ${}_TG^\circ$) of energy relevant to the optimized structure, zero-point energy and Gibbs free energy contribution were computed by the program. Values of ${}_TH^\circ$, ${}_TS^\circ$ and ${}_TG^\circ$ were subsequently used to predict enthalpy ($\Delta_{r,T}H^\circ$) and Gibbs free energy ($\Delta_{r,T}G^\circ$) differences for consecutive steps of the decomposition of $CaC_2O_4{\cdot}H_2O$ at a given temperature and a standard pressure (°), as well as the relevant activation characteristics: $\Delta_{a,T}H^\circ$, $\Delta_{a,T}S^\circ$, and $\Delta_{a,T}G^\circ$, by following the basic rules of thermodynamics [21].

Results and discussion

Decomposition pathway on the basis of computation results

The decomposition pathway was explored taking into account the results of thermal analysis and other investigations, on the basis of which it is known that solid $CaC_2O_4{\cdot}H_2O$ decomposes in three steps [1–9]:

$$\begin{aligned} CaC_2O_4 \cdot H_2O_{(s)} \xrightarrow{\text{step I}} & \uparrow H_2O_{(g)} + CaC_2O_{4(s)} \xrightarrow{\text{step II}} \\ & \uparrow CO_{(g)} + CaCO_{3(s)} \xrightarrow{\text{step III}} \\ & \uparrow CO_{2(g)} + CaO_{(s)} \end{aligned} \quad (1)$$

We assumed that in the situation when all reactants are gaseous, the compound also decomposes in the three steps shown in relationship (1). Geometry optimizations of all the reactants lead to stationary points corresponding to the lowest-energy structures. Such optimizations in the case of three transition states lead to stationary points on the decomposition pathway. Enthalpies and Gibbs free energies corresponding to molecular states during $CaC_2O_4{\cdot}H_2O$ decomposition are presented in Fig. 1, while geometries of calcium-containing entities in the lowest-energy and transition states are shown in Fig. 2.

Computational data indicate that the general scheme for the decomposition of solid calcium oxalate monohydrate matches well that for the dissociation of the gaseous compound. In the latter conditions, decomposition is predicted to be a three-step endothermal, forced process. This arises from the fact that $\Delta_{r,298}H^\circ$ and $\Delta_{r,298}G^\circ$ (Fig. 1) take positive values (the enthalpies of reactions are more positive, since the entropies of reactions, always positive, lower the values of $\Delta_{r,298}G^\circ$). All three steps need to overcome activation barriers, which are the highest for decarbonylation (step II) and lowest for dehydration (step I). Figure 2 shows molecular structures of the lowest-energy entities containing Ca and those in transition states corresponding to dehydration, decarbonylation and decarboxylation. When molecular changes during the reaction are substantial, one can expect higher activation barriers: this is the case with decarbonylation (step II). Thermodynamic (corresponding to equilibrium) and activation (corresponding to non-equilibrium conditions) characteristics will be used in the analysis of the behaviour of continuously heated molecular systems, to which we now proceed.

Thermal behaviour across temperature

Endothermal/forced processes require a supply of energy/Gibbs free energy to transform chemical systems from the substrate side to the product side. Thermally forced processes are usually initiated by a supply of heat in the temperature range in which the products occur. To gather information on this latter feature or, in other words, the thermal reactivity of $CaC_2O_4{\cdot}H_2O$, we plotted values of $\Delta_{r,T}G^\circ$ versus temperature for three decomposition steps (Fig. 3). When $\Delta_{r,T}G^\circ$ is positive, substrates prevail, but when it is negative, products do so (below the line $\Delta_{r,T}G^\circ = 0$). The line $\Delta_{r,T}G^\circ = 0$ represents equilibrium between reactants.

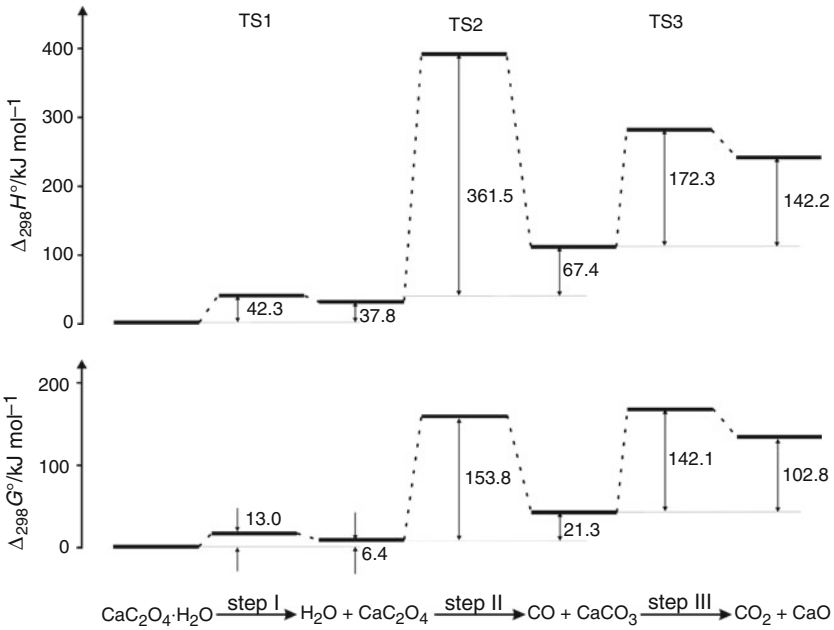

Fig. 1 Enthalpy (*upper graph*) and Gibbs free energy (*lower graph*) changes (in kJ mol^{-1}) along the multistep decomposition pathway of isolated calcium oxalate monohydrate at ambient temperature and standard pressure

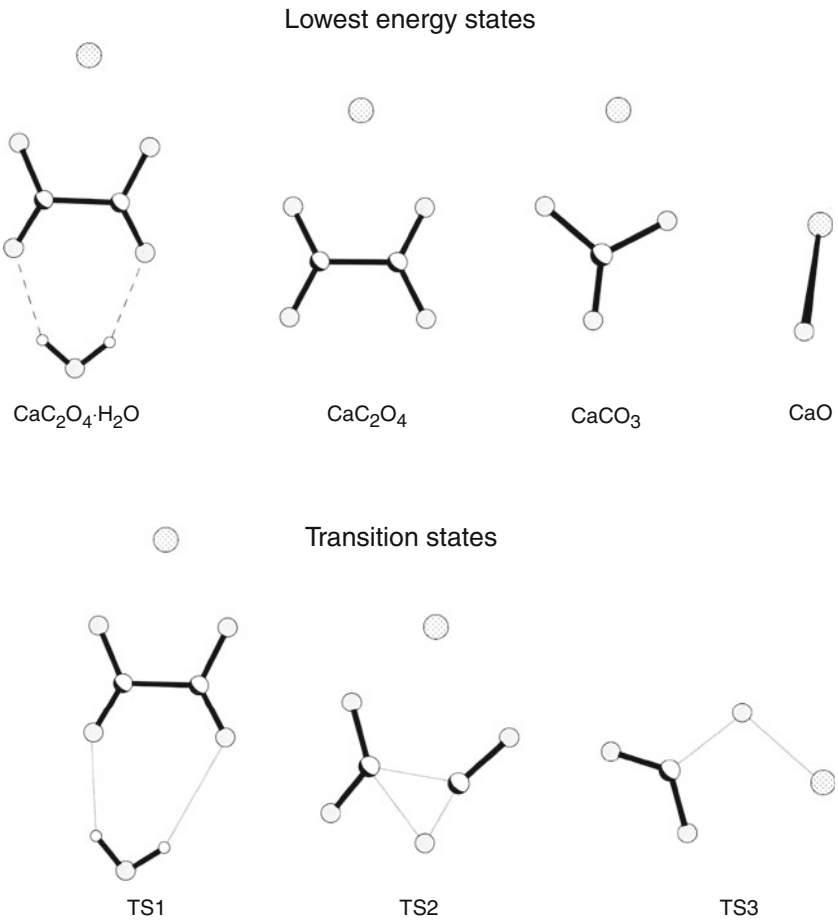

Fig. 2 Geometries of calcium-containing entities (indicated in Fig. 1) occurring along the multistep decomposition pathway of isolated calcium oxalate monohydrate (*dashed lines* represent H-bonds, *solid lines* bonds that are broken or formed when a transition state is crossed)

$\Delta_{r,T}G°$ is related to the equilibrium constant ($_TK°$) by the phenomenological dependence (2),

$$\Delta_{r,T}G° = -RT \ln_T K° \quad (2)$$

in which R denotes the gas constant. For the processes shown in relationship (1) there is only one gaseous product in each reaction step. In such a case, $_TK° = p/p°$, where

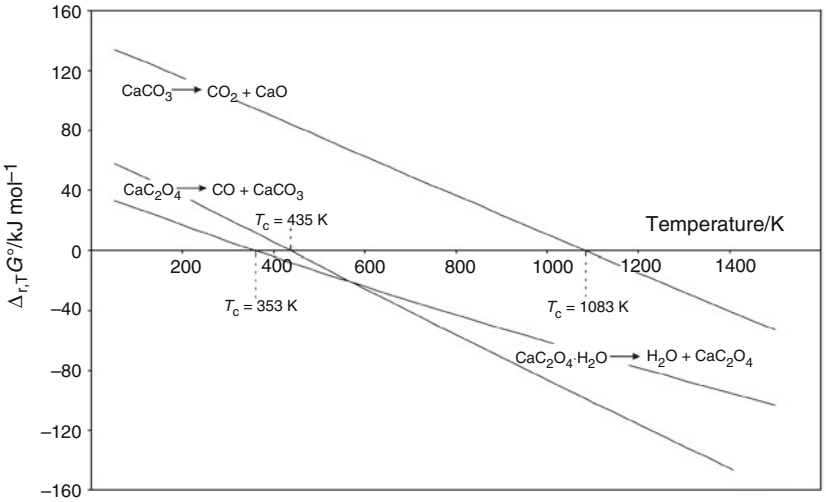

Fig. 3 Temperature relationships of Gibbs free energy for the consecutive steps of the decomposition of gaseous calcium oxalate monohydrate

p is the equilibrium vapour pressure of the gaseous product at a given temperature (T) and $p°$ the standard pressure. If thermal processes are carried out in a system open to the atmosphere (as in typical thermal analysis experiments), p can only reach $p°$, which corresponds to the situation in which ${}_{T}K° = 1$ and $\Delta_{r,T}G° = 0$. Under such experimental conditions, therefore, $\Delta_{r,T}G°$ never reaches negative values. Decomposition is completed at the instant $\Delta_{r,T}G°$ reaches 0. In our theoretical analyses there are always three gaseous reactants whose equilibrium vapour pressures determine ${}_{T}K°$ values, which are in turn related to $\Delta_{r,T}G°$ by expression (2). In this situation, the features of both ${}_{T}K°$ and $\Delta_{r,T}G°$ should resemble those characterizing the decomposition of solid $CaC_2O_4 \cdot H_2O$, i.e. decomposition should be complete at ${}_{T}K° = 1$ or when $\Delta_{r,T}G°$ reaches 0. Bearing in mind these latter assumptions, decomposition completion temperatures (T_c) for the dehydration, decarbonylation and decarboxylation of $CaC_2O_4 \cdot H_2O$ were found to be 353, 435 and 1,083 K, respectively (Fig. 3).

Thermal equilibria across temperature

The equilibrium constants resulting from Eq. (2) and given by relationship ${}_{T}K° = \exp\left[-\Delta_{r,T}G°/(RT)\right]$ are in reality equal to the extent of reaction (α), as reflected by thermal analysis data for a given reaction step. $\Delta_{r,T}G°$ values (Fig. 3) were thus used to predict equilibrium values of α across temperature, starting from the lowest temperature and finishing at the completion temperature for each reaction step.

Thermal gravimetry data combine the effects of all thermal processes that occur when temperature increases. So as to facilitate comparison of experimental and computational TG data we standardized the results of computations by assuming the total mass to be 1.000. Then, the mass losses corresponding to the three reaction steps in relation to the total mass are (the values in parentheses represent α for a given step): 1.000 (0.000)–0.877 (1.000), dehydration; 0.877 (0.000)–0.685 (1.000), decarbonylation; 0.685 (0.000)–0.384 (1.000), decarboxylation. Combined in this way, the values of α for the three reaction steps are shown in Fig. 4 as a solid line; this represents the pattern of the predicted TG curve for the stepwise decomposition of $CaC_2O_4 \cdot H_2O$ in equilibrium conditions.

Kinetic phenomena during decomposition

The thermal equilibria considered in the previous section could be achieved if forced processes were not required to overcome activation barriers. Examples of such processes are first-order phase transitions. Chemical processes usually need to overcome activation barriers and thus proceed in non-equilibrium conditions. Information on the chemical changes (extent of reaction) in such conditions can be obtained from kinetic relationships, which are briefly described below.

The basic kinetic equation for unimolecular decomposition,

$$\mathrm{A} \rightarrow \mathrm{B} + \mathrm{C} \tag{3}$$

which takes the differential form

$$-\mathrm{d}c_\mathrm{A}/\mathrm{d}t = c_\mathrm{A}k(T) \tag{4}$$

can be converted after integration to the form

$$\ln c_{0\mathrm{A}}/c_\mathrm{A} = tk(T) \tag{5}$$

where A, B, C represent reactants, c_A and $c_{0\mathrm{A}}$ respectively denote current and initial concentrations, t is time and $k(T)$ is the rate constant. If we substitute $1 - \alpha$ (which results from the relationship $\alpha = c_{0\mathrm{A}} - c_\mathrm{A}/c_{0\mathrm{A}}$) in place of $c_\mathrm{A}/c_{0\mathrm{A}}$, we obtain the integral kinetic equation in the form containing the extent of reaction instead of the concentration (not well defined in thermal analysis experiments) [22]

$$-\ln(1-\alpha) = tk(T) \tag{6}$$

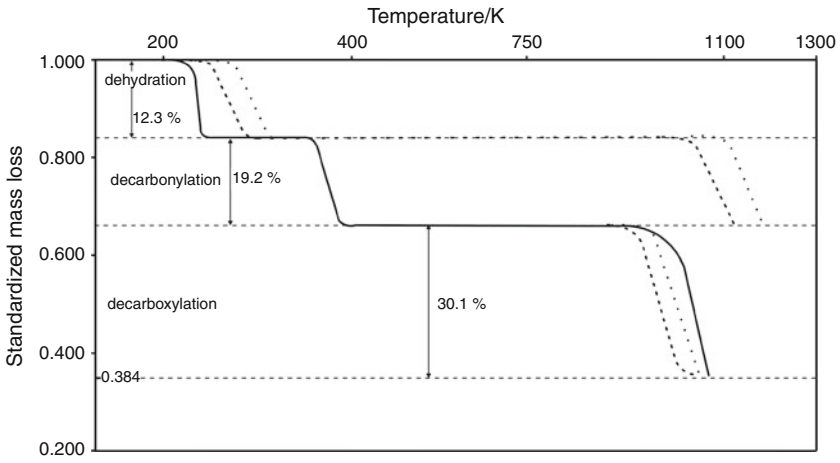

Fig. 4 Predicted equilibrium (*solid line*) and non-equilibrium (*dashed line* heating rate 5 K min^{-1}, *dotted line* heating rate 25 K min^{-1}) profiles for the decomposition of $CaC_2O_4{\cdot}H_2O$

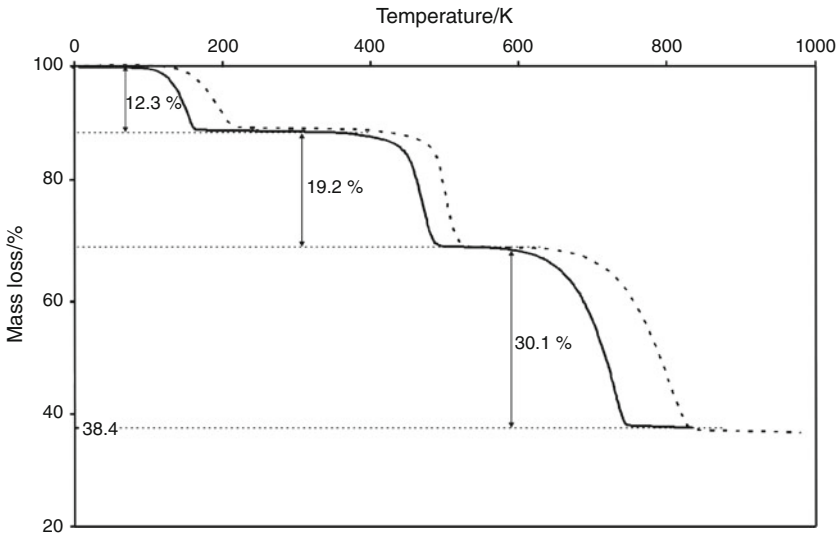

Fig. 5 Experimental TG curves reflecting the decomposition of $CaC_2O_4{\cdot}H_2O$ at two heating rates: 5 K min^{-1} (*solid line*) and 25 K min^{-1} (*dashed line*)

The adaptation of kinetic equations to non-isothermal conditions has been discussed in detail elsewhere [22, 23]. Here, only the final results are invoked, which can be presented as follows. In non-isothermal analysis, as in our case, time can be replaced by T/Φ (where Φ represents heating rate), which is possible when Φ changes linearly: $\Phi = \mathrm{d}T/\mathrm{d}t$ (integration of this relationship leads to $t = T/\Phi$ [22]). For the rate constant, the equation derived from transition state theory seems best suited [21]:

$$k(T) = [RT/(Nh)] \exp(\Delta_{a,T}S^{\circ}/R) \exp[-\Delta_{a,T}H^{\circ}/(RT)] \quad (7)$$

where h stands for Planck's constant and N is the Avogadro number. Combining Eqs. (6) and (7) yields a relationship for α (8):

$$\alpha = 1 - \exp\{-(T/\Phi)[RT/(Nh)] \exp(\Delta_{a,T}S^{\circ}/R) \exp[-\Delta_{a,T}H^{\circ}/(RT)]\} \quad (8)$$

which was used to predict values of α for each reaction step. These values were then plotted in Fig. 4 using the scheme described in the previous section. In these calculations we assumed the predicted values of $\Delta_{a,T}S^{\circ}$ and $\Delta_{a,T}H^{\circ}$.

The dashed and dotted lines in Fig. 4 represent the pattern of predicted TG curves for the stepwise decomposition of $CaC_2O_4{\cdot}H_2O$ in non-equilibrium conditions.

Predicted versus experimental decomposition patterns

The predicted dissociation pattern of $CaC_2O_4{\cdot}H_2O$ (Fig. 4) in equilibrium conditions and that reflected by TG curves (Fig. 5) are similar and characteristic of three consecutive, non-overlapping decomposition steps. There are, however, differences in the location of the thermal effect signals on the temperature scale. According to predictions, dehydration and decarboxylation should proceed at higher temperatures than the TG data indicate, whereas decarbonylation is predicted to take place over a lower temperature range than that resulting from TG data.

The reaction profiles predicted for the decomposition of $CaC_2O_4{\cdot}H_2O$ in non-equilibrium conditions (Fig. 4) using

relationship (8) do not match the experimental TG data (Fig. 5). According to kinetic predictions, dehydration, the signal of which should occur first when the temperature increases, should be followed by the signals of decarboxylation and then decarbonylation. The unexpected effect has occurred because the activation barriers predicted for decarbonylation are much higher than those for decarboxylation. This seems to be an obvious deficiency of the molecular model (i.e. entities originating from a stoichiometric unit of $CaC_2O_4{\cdot}H_2O$ in the gaseous phase) adopted in the calculations.

It is evident from both experimental and computational data that increasing the heating rate shifts the curves reflecting mass loss to higher temperatures. From computational data it also emerges that the curves representing mass loss in equilibrium conditions lie at lower temperatures relative to the ones reflecting mass loss in non-equilibrium conditions. This latter finding, seen in the cases of dehydration and decarbonylation, is a logical consequence of the fact that under equilibrium conditions molecular systems have to overcome only thermodynamic barriers for a process to proceed, whereas in non-equilibrium conditions, kinetic (activation) barriers have to be surmounted, and these are always higher.

Conclusions

The results of this study show that computational methods are a convenient tool for analysing the thermal processes taking place as temperature rises. These methods provide insight into the molecular changes occurring when substrates are converted to products and enable the thermodynamic and kinetic characteristics of the various processes to be determined.

It has been demonstrated that, on the basis of fundamental thermodynamic and kinetic relationships, it is possible to generate reaction profiles representing mass loss during the continuous heating of $CaC_2O_4{\cdot}H_2O$, which in certain cases qualitatively match experimental TG data. The agreement is reasonable given that the computations applied to the gaseous phase and the experiments related to systems in which all Ca-containing entities were in the solid state.

Comparison of the data obtained in this study and those presented in our earlier paper on a similar subject [1] leads to the conclusion that in both cases the decomposition pathway of calcium oxalate monohydrate is predicted to be the same and is consistent with experimental findings. The thermodynamic data presented here (Fig. 1) compare somewhat better with the experimental values than the computational data that we predicted earlier (Table 2 in Ref. [1]). In the present study, we took a different approach for predicting the decomposition profiles than the one used in Ref. [1]. As a result, the decomposition pattern of $CaC_2O_4{\cdot}H_2O$ predicted here (Fig. 4) is much closer to the experimental one (Fig. 5) than the pattern predicted and reported in our previous work (Fig. 2 in Ref. [1]). Here, moreover, we predicted the decomposition profiles under equilibrium and non-equilibrium conditions, whereas earlier this was done only under equilibrium conditions.

The agreement between computational and experimental characteristics would undoubtedly improve if entities from the environment were included in the quantum chemistry calculations. Our preliminary results indicate that thermodynamic and activation barriers are lower when a non-reacting molecule accompanies a reacting one. The latter finding opens up prospects for further investigations, which may require much more time owing to the substantial increase in the size of objects studied.

Acknowledgements This study was financed by the State Funds for Scientific Research (Grant DS/8220-4-0087-1). The authors would like to thank Mrs Gabriela Wiczk and Mrs Estera Hebanowska for their contribution to the TG measurements. The MP2 calculations were carried out at the Academic Computer Centre in Gdańsk (TASK) and the Wrocław Centre for Networking and Supercomputing (WCSS).

References

1. Rak J, Skurski P, Gutowski M, Błażejowski J. Thermodynamics of the thermal decomposition of calcium oxalate monohydrate examined theoretically. J Therm Anal. 1995;43:239–46.
2. Kutaish N, Aggarwal P, Dollimore D. Thermal analysis of calcium oxalate samples obtained by various preparative routes. Thermochim Acta. 1997;297:131–7.
3. Mianowski A. J Therm Anal Calorim. 2001;63:765–76.
4. Gao Z, Amasaki I, Nakada M. A description of kinetics of thermal decomposition of calcium oxalate monohydrate by means of the accommodated Rn model. Thermochim Acta. 2002;385:95–103.
5. Liqing L, Donghua C. Application of iso-temperature method of multiple rate to kinetic analysis. J Therm Anal Calorim. 2004; 78:283–93.
6. Frost RL, Weier ML. Thermal treatment of whewellite—thermal analysis and Raman spectroscopic study. Thermochim Acta. 2004; 409:79–85.
7. Vlaev L, Nedelchev N, Gyurova K, Zagorcheva M. A comparative study of non-isothermal kinetics of decomposition of calcium oxalate monohydrate. J Anal Appl Pyrolysis. 2008;81:253–62.
8. Perez-Rodriguez JL, Duran A, Centeno MA, Martinez-Blanesa JM, Robador MD. Thermal analysis of monument patina containing hydrated calcium oxalates. Thermochim Acta. 2011;512: 5–12.

9. Mianowski A, Baraniec-Mazurek I, Bigda R. Some remarks on equilibrium state in dynamic condition. J Therm Anal Calorim. 2012;107:1155–65.
10. Mao Y, Siders PD. Molecular Hartree–Fock model of calcium carbonate. J Mol Struct (Theochem). 1997;419:173–84.
11. Di Tommaso D, de Leeuw NH. Theoretical study of the dimerization of calcium carbonate in aqueous solution under natural water conditions. Geochim Cosmochim Acta. 2009;73:5394–405.
12. Møller C, Plesset MS. Note on an approximation treatment for many-electron systems. Phys Rev. 1934;46:618–22.
13. Davidson E, Feller D. Basis set selection for molecular calculations. Chem Rev. 1986;86:681–96.
14. Dunning TH. Gaussian basis sets for use in correlated molecular calculations. I. The atoms boron through neon and hydrogen. J Chem Phys. 1989;90:1007–23.
15. Frish MJ, Trucks GW, Schlegel HB, Scuseria GE, Robb MA, Cheeseman JR, et al. Gaussian 09, revision B.01. Wallingford: Gaussian, Inc; 2009.
16. Tazzoli V, Domeneghetti MC. The crystal structures of whewellite and weddellite: re-examination and comparison. Am Mineral. 1980;65:327–34.
17. Hochrein O, Thomas A, Kniep R. Revealing the crystal structure of anhydrous calcium oxalate, $Ca[C_2O_4]$, by a combination of atomistic simulation and rietveld refinement. Z Anorg Allgem Chem. 2008;634:1826–9.
18. Brik MG. First-principles calculations of structural, electronic, optical and elastic properties of magnesite $MgCO_3$ and calcite $CaCO_3$. Physica B Condens Matter. 2011;406:1004–12.
19. Hehre WJ, Radom L, von Schleyer PR, Pople JA. Ab initio molecular orbital theory. New York: Wiley; 1986.
20. Dewar MJS, Ford GP. Ground states of molecules. 44. MINDO/3 calculations of absolute heat capacities and entropies of molecules without internal rotations. J Am Chem Soc. 1977;99:7822–9.
21. Atkins PW, de Paula J, editors. Atkins' physical chemistry. 7th ed. Oxford: Oxford University Press; 2006.
22. Błażejowski J. Remarks on the description of reaction kinetics under non-isothermal conditions. Thermochim Acta. 1984;76:359–72.
23. Błażejowski J. Evaluation of kinetic constants for the solid state reactions under linear temperature increase conditions. Thermochim Acta. 1981;48:109–24.